

AD-A038 782

AIR FORCE GEOPHYSICS LAB HANSCOM AFB MASS  
POLARIZATION SPECTRA OF CENTIMETER WAVELENGTH SOLAR BURSTS USIN--ETC(U)  
DEC 76 D A GUIDICE

F/G 3/2

UNCLASSIFIED

AFGL-TR-76-0295

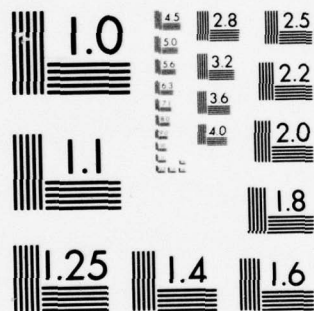
NL

| OF |  
AD  
A038782



END

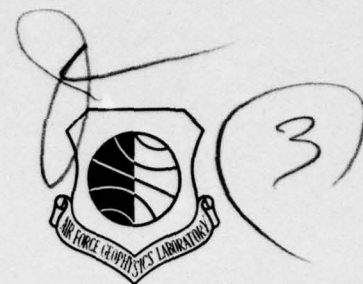
DATE  
FILMED  
5-77



MICROCOPY RESOLUTION TEST CHART  
NATIONAL BUREAU OF STANDARDS-1963-A

ADA 038782

AFGL-TR-76-0295  
ENVIRONMENTAL RESEARCH PAPERS, NO. 585

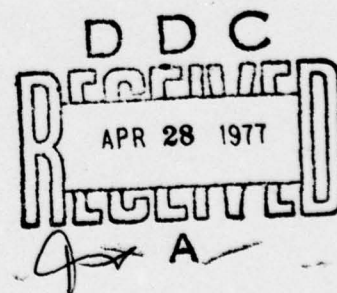


## Polarization Spectra of Centimeter-Wavelength Solar Bursts Using Whole-Sun Observations

DONALD A. GUIDICE

8 December 1976

Approved for public release; distribution unlimited.



SPACE PHYSICS DIVISION    PROJECT 4643  
**AIR FORCE GEOPHYSICS LABORATORY**  
HANSOM AFB, MASSACHUSETTS 01731

**AIR FORCE SYSTEMS COMMAND, USAF**



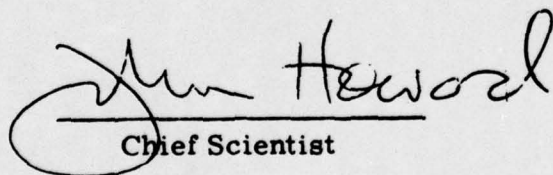
AD No. /  
DDC FILE COPY

✓

This report has been reviewed by the ESD Information Office (OI) and is releasable to the National Technical Information Service (NTIS).

This technical report has been reviewed and is approved for publication.

FOR THE COMMANDER

  
Chief Scientist

Qualified requestors may obtain additional copies from the Defense Documentation Center. All others should apply to the National Technical Information Service.



Unclassified

SECURITY CLASSIFICATION OF THIS PAGE (When Data Entered)

REPORT DOCUMENTATION PAGE		READ INSTRUCTIONS BEFORE COMPLETING FORM
1. REPORT NUMBER AFGL-TR-76-0295, AFGL-ERP-585	2. GOVT ACCESSION NO.	3. RECIPIENT'S CATALOG NUMBER
4. TITLE (and Subtitle) POLARIZATION SPECTRA OF CENTIMETER- WAVELENGTH SOLAR BURSTS USING WHOLE- SUN OBSERVATIONS,	5. TYPE OF REPORT & PERIOD COVERED Scientific. Interim.	
7. AUTHOR(s) Donald A. Guidice	6. PERFORMING ORG. REPORT NUMBER ERP No. 585	
9. PERFORMING ORGANIZATION NAME AND ADDRESS Air Force Geophysics Laboratory (PH) Hanscom AFB Massachusetts 01731	8. CONTRACT OR GRANT NUMBER(s)	
11. CONTROLLING OFFICE NAME AND ADDRESS Air Force Geophysics Laboratory (PH) Hanscom AFB Massachusetts 01731	10. PROGRAM ELEMENT, PROJECT, TASK AREA & WORK UNIT NUMBERS 62101F 46430301	
14. MONITORING AGENCY NAME & ADDRESS (if different from Controlling Office)	12. REPORT DATE 8 Dec 1976	
	13. NUMBER OF PAGES 36	
	15. SECURITY CLASS. (of this report) Unclassified	
15a. DECLASSIFICATION/DOWNGRADING SCHEDULE		
16. DISTRIBUTION STATEMENT (of this Report) Approved for public release; distribution unlimited.		
17. DISTRIBUTION STATEMENT (of the abstract entered in Block 20, if different from Report)		
18. SUPPLEMENTARY NOTES		
19. KEY WORDS (Continue on reverse side if necessary and identify by block number) Polarization spectra Centimeter-wavelength bursts Whole-sun observations 5 to 9.4 GHz polarization measurements Sagamore Hill Radio Observatory Solar radio-burst polarization		
20. ABSTRACT (Continue on reverse side if necessary and identify by block number) Data on the intensity and circular polarization of solar bursts at 9.4 GHz and 7 GHz are obtained from daily sunrise-to-sunset patrols carried out by the Instituto Geofisico del Peru and MacKenzie University under AFGL-sponsored AFOSR grants. In-house observations of the four Stokes polarization parameters at 5 GHz have been carried out on a limited patrol basis at the Sagamore Hill Radio Observatory. The input from the three frequencies has been combined to obtain circular-polarization spectral data on a small number of cm-λ solar bursts.		

DD FORM 1 JAN 73 1473 EDITION OF 1 NOV 65 IS OBSOLETE

Unclassified

SECURITY CLASSIFICATION OF THIS PAGE (When Data Entered)

409 578

Unclassified

SECURITY CLASSIFICATION OF THIS PAGE(When Data Entered)

20. Abstract (Continued)

The physics of microwave-burst emission is briefly examined to give the rationale for investigating polarization spectra. The instruments used to carry out the 9.4 GHz and 7 GHz circular-polarization measurements and the 5 GHz Stokes-parameter measurements are described.

A survey of the August 1972 to December 1973 period produced a table of 45 bursts, from which some limited results were obtained. About 75 to 80 percent of all bursts are circularly polarized, with varying polarization over the 5 to 9.4 GHz range. For most bursts where the circular polarization  $p_c$  increases toward the upper or lower end of the 5 to 9.4 GHz range, the total intensity  $I$  also increases in that direction. The few bursts having a  $p_c$  sense reversal in the 5 to 9.4 GHz range also have a spectral maximum of  $I$  at roughly the same frequency. Some simplified explanations of the results are presented.

ACCESSION FOR	
DTIC	WHICH SECTION <input checked="" type="checkbox"/>
DDC	WHICH SECTION <input type="checkbox"/>
UNANNOUNCED	<input type="checkbox"/>
JUSTIFICATION	
BY	
DISTRIBUTION/AVAILABILITY	
Dist.	Avail. 400/94
A	

Unclassified

SECURITY CLASSIFICATION OF THIS PAGE(When Data Entered)

## Preface

The fullest acknowledgment is due Mr. Carl Ferioli for his outstanding effort in the construction of the three-antenna mount and solar tracker, the fabrication of the r-f instrumentation, and the wiring of complex equipment within the trailer. Without Mr. Ferioli's expert help in these areas, the development of the Sagamore Hill 5-GHz solar polarization instrument would never have been accomplished. The author also acknowledges the effort of MSgt. Cecil Hull in the operation and maintenance of the 5 GHz instrument at Sagamore Hill and the compilation of data from both the in-house 5 GHz observations and the 7 and 9.4 GHz contractor observations.

Acknowledgment is also due to personnel of the Instituto Geofisico del Peru (Huancayo Observatory), especially to Dr. Mutsumi Ishitsuka, the principal investigator for the 9.4 GHz polarization work, and Dr. Alberto Giesecke, Director of the Institute, and to personnel at Universidade Mackenzie (Itapetinga Observatory), especially Dr. Paulo Marques dos Santos, the principal investigator for the 7 GHz polarization work, and Dr. Pierre Kaufmann, Director of CRAAM (Centro de Radio-Astronomia e Astrofisica Mackenzie) and the previous principal investigator.

Finally, the author is indebted to Mr. John Castelli for the radio-patrol instrumentation he developed at Sagamore Hill that served as a model for much of the 5 GHz polarization instrumentation, and for the continued interest and encouragement he has given the solar polarization program.

## Contents

1. INTRODUCTION	7
2. SPECTRA AND POLARIZATION OF MICROWAVE BURSTS	11
2.1 Spectra of cm- $\lambda$ Bursts	11
2.2 Polarization of cm- $\lambda$ Bursts	13
3. WHOLE-SUN cm- $\lambda$ POLARIZATION MEASUREMENTS	17
3.1 Circular-Polarization Instrumentation at 9.4 and 7 GHz	17
3.2 Sagamore Hill 5 GHz Polarization Instrumentation	19
4. RESULTS OF POLARIZATION SPECTRA OBSERVATIONS	25
4.1 Polarization-Patrol Burst Survey	25
4.2 Results and Discussion	30
REFERENCES	35

## Illustrations

1. Idealized Peak Flux Density Spectrum of a Radio Burst (representative of actual burst spectra) Used for Spectral Classification	12
2. Percentage Distribution of the Observed Spectral Maxima of Bursts With C Type Spectra (Sagamore Hill data, 1968-1971)	13
3. Radiated Power Spectra (theoretically computed) at Various Observation Angles $\theta$ for a Group of Energetic Electrons Having a Power-Law Energy Distribution With $\Gamma = 2$ and an Energy Range of 100 to 1000 keV	14



## Illustrations

4. Theoretical Curves of Circular and Linear Polarization Resulting From Mode-Coupling Transformation in the QT-Region Above a Solar Burst	16
5. Block Diagram of the Instrumentation Used at the Huancayo Observatory to Measure the Circular Polarization and Total Intensity of Solar Emission at 9.4 GHz	20
6. Antenna and Equatorially Mounted Tracker Used for 9.4 GHz Solar Polarization Observations at Huancayo Observatory	21
7. Radiometer "Back End" Components in the Receiver Building at the Huancayo Observatory	21
8. Antenna and Equatorially Mounted Tracker Used for 7 GHz Solar Polarization Observations at Itapetinga Observatory	22
9. Radiometer "Back End" Components in the Receiver Building at the Itapetinga Observatory	22
10. Block Diagram of the Sagamore Hill 5 GHz Radiometric Instrumentation Capable of Measuring the Four Stokes Parameters of Polarization	23
11. Three Antennas and Instrument Box on Equatorially Mounted Solar Tracker Used for 5 GHz Solar Polarization Observations at the Sagamore Hill Radio Observatory	25
12. Tracker Control Panel and Radiometer "Back End" Components Housed in a Trailer Used for 5 GHz Polarization Observations at Sagamore Hill	25

## Tables

1. Geographic and Instrumentation Parameters of Polarization-Study Stations	26
2. Parameters of Bursts Used in Polarization Spectra Study	28

## Polarization Spectra of Centimeter-Wavelength Solar Bursts Using Whole-Sun Observations

### I. INTRODUCTION

The polarization of solar radio emission was first noted as far back as 1946, when circular polarization of noise-storm radiation from large active regions was observed.<sup>1</sup> The polarization properties of meter-wavelength radiation (morphologically, the type I to V bursts) have been detailed in several comprehensive texts.<sup>2,3</sup>

In the centimeter-wavelength (cm- $\lambda$ ) range, the polarized portion of burst radiation was observed to be circular. Certain observations of linear or elliptical polarization reported in the early literature were found to be of questionable accuracy upon later examination. If linear polarization is present at the source of a solar burst, its actual observed value would probably be greatly reduced by dispersive coronal propagation effects. Observations of the circular polarization of

---

(Received for publication 2 December 1976)

1. Pawsey, J. L., and Bracewell, R. N. (1955) Radio Astronomy, Oxford Univer. Press, Oxford, p. 185.
2. Kraus, J. D. (1966) Radio Astronomy, McGraw-Hill, New York, p. 338.
3. Zheleznyakov, V. V. (1970) Radio Emission of the Sun and Planets, Permagon Press, Oxford, pp. 238-240.



solar emissions have been made at  $\text{cm-}\lambda$ , using both high-resolution<sup>4</sup> and low-resolution (whole-sun)<sup>5</sup> instruments.

At the Sagamore Hill Radio Observatory, routine whole-sun observations of the flux density of the quiet sun and bursts are made at nine fixed frequencies covering the 245 to 35000 MHz range.<sup>6</sup> The major portion of the in-house analytic research on solar bursts is based on data from these observations. Because of the wide range of frequency coverage, emphasis is placed on spectral (flux density vs frequency) characteristics of the bursts. Spectral analyses have included both the statistical properties of the peak flux density of large numbers of mainly small bursts<sup>7</sup> and the time-development of the spectra of a few large bursts.<sup>8</sup>

In establishing the burst polarization program, it was decided to use certain approaches similar to those employed in the Sagamore Hill flux density measurements program. Routine whole-sun multifrequency patrols would be used with operation (initially, at least) in the  $\text{cm-}\lambda$  range. Since circular polarization of  $\text{cm-}\lambda$  bursts was well established, the effort to obtain spectral data would concentrate on circular polarization measurements, although a limited effort at trying to measure linear polarization (at one frequency, for example) would be made.

Data on the total intensity (flux density) and circular polarization of quiet-sun emission and bursts have been sent monthly to AFGL by Mackenzie University, Sao Paulo, Brazil (starting in 1968), and by Instituto Geofisico del Peru, Lima, Peru (starting in 1969). These efforts are supported by AFGL through AFOSR grants. In both cases, data are obtained from routine daily single-frequency whole-sun patrols, with antenna beamwidths many times the sun's angular diameter to insure accurate flux density measurements. Mackenzie's observations are made at 7.0 GHz (4.3  $\text{cm } \lambda$ ) at the Itapetinga Radio Observatory; IGP's observations are made at 9.4 MHz (3.2  $\text{cm } \lambda$ ) at the Huancayo Observatory.

The distribution of the peak flux-density spectra of  $\text{cm-}\lambda$  bursts showed that the observed spectral maximum ( $f_{\text{max}}$ ) of the greatest number of bursts occurred at the 4995 MHz (C-band) patrol.<sup>7</sup> (The actual crest of the  $f_{\text{max}}$  distribution was

4. Richards, D.W., and Straka, R.M. (1971) Solar polarization mapping at 7.8 GHz, Nature, Phys. Sci., 233:92.
5. Ishitsuka, M. (1975) Solar Patrol at 9400 MHz, Final Scientific Report, Instituto Geofisico del Peru, AFGL-TR-76-0050.
6. Castelli, J.P., Aarons, J., Guidice, D.A., and Straka, R.M. (1973) The solar radio patrol network of the USAF and its application, Proc. IEEE, 661:1307.
7. Guidice, D.A., and Castelli, J.P. (1975) Spectral distribution of microwave bursts, Solar Phys., 44:155.
8. Castelli, J.P., Guidice, D.A., and Aarons, J. (1975) Comparison of morphology and spectra of August 7, 1972 outburst at microwave and hard x-rays, presented at XVII Gen. Assembly of URSI, Lima, Peru, 11-15 August 1975.

determined to be about 6.5 GHz). It was decided to make the in-house polarization observations at 5 GHz (6 cm  $\lambda$ ), roughly the same frequency as the Sagamore Hill flux density patrol. The polarization instrumentation was to be capable of measuring the complete set of polarization parameters (not just circular polarization). However, since circular polarization measurements are routinely made at 7 GHz and 9.4 GHz at longitudes not too different from that of Sagamore Hill (Itapetinga is about 20° east of Sagamore Hill's longitude, Huancayo about 5° west), it was decided that the Sagamore Hill instrumentation would be capable of giving unambiguous circular polarization data at 5 GHz, so as to obtain the circular polarization spectra of bursts over the 5 to 9.4 GHz range.

The most general case of polarization is partially polarized radiation, which consists of the completely polarized portion (elliptically polarized for the most general case) and the unpolarized (or randomly polarized) portion. The polarized portion is characterized by its intensity  $I_p$ , the axial ratio  $r$  (the sign of  $r$  indicating the sense), and the orientation angle  $\chi$  of the ellipse; the unpolarized portion is characterized by one parameter, its intensity  $I_u$ . Thus, four parameters are required to define the general case of partially polarized radiation. These parameters are given in various sets: one of the most common is  $I$ ,  $I_p$ ,  $r$ , and  $\chi$ , where the total intensity  $I = I_p + I_u$ .

The four parameters of polarization could be measured using a single aperture and a fixed dual-polarized feed. This requires processing involving multiplication or correlation of voltages. Crosstalk (between opposite antenna polarizations) and other multiplicative effects introduce apparent (erroneous) polarization into the system. For example, if it were attempted to measure linear polarization using one antenna with dual circularly polarized reception, system crosstalk of -20 dB could cause the apparent measurement of 20 percent polarization for the reception of unpolarized incident radiation. The error expression, given by Cohen,<sup>9</sup> is  $m_e = 2|k|$ , where  $m_e$  is the erroneous polarization and  $k$  is the crosstalk voltage ratio (that is,  $\text{dB} = 20 \log_{10} k$ ). Even crosstalk limited to -30 dB would lead to an erroneous 6 percent polarization. Since any real linear polarization of solar polarization is at best very small (<6 percent), the use of such a system to detect linear polarization would lead to ambiguous and questionable results.

For the 5 GHz observations, it was decided to measure the complete set (four) of polarization parameters by methods not involving voltage multiplication or correlation; that is, by methods involving only the measurement of sums and differences of incident power. On this basis, we seek to measure the four Stokes parameters of polarization:

9. Cohen, M.H. (1958) The Cornell radio polarimeter, Proc. IRE, 46:183.

$$I = \text{total intensity } (I_p + I_u)$$

$$Q = I_x - I_y$$

$$U = I_t - I_s$$

$$V = I_l - I_r$$

where  $I_x$  and  $I_y$  are the intensities measured using a dual linearly polarized antenna with horizontal/vertical orientation,  $I_t$  and  $I_s$  are the intensities measured using a dual linearly polarized antenna with  $45^\circ/135^\circ$  orientation, and  $I_l$  and  $I_r$  are the intensities measured using a dual circularly polarized (left/right) antenna. The total intensity  $I$  of any radiation (partially polarized being the most general case) can be obtained by taking the sum of any two orthogonally polarized components:

$$I = I_x + I_y = I_t + I_s = I_l + I_r \quad .$$

Consideration was given to using one antenna and time-sharing the aperture among various polarizations using mechanical rotation of linear dipoles and the switching in and out of a phase delay hybrid (to give left and right circular polarization). However, the mechanical problems involved might have led to difficulties in operating the system on a routine basis.

The arrangement finally decided upon for Sagamore Hill utilized three 6-ft parabolic antennas on a common mount (solar tracker). Each of the antennas was polarized and oriented so that it permitted measurement of one of the Stokes parameters involving a difference in incident power ( $Q$ ,  $U$ , or  $V$ ). A comparison-feed mode of operation using a modulator switch was employed. The Stokes parameter  $I$  of the solar emission could be obtained from the sum of any two orthogonally polarized measurements (that is, from any of the three antennas) using a comparison-load mode of operation (employing another modulator switch). However, the addition of this comparison-load switch to any of the comparison-feed systems imposes a factor-of-two sensitivity penalty on that system. Since the linear polarization from solar radiation is expected to be much smaller than circular polarization and since the linear-polarization systems would have much poorer sensitivity (due to the narrower bandwidth needed to limit Faraday-rotation dispersion), the comparison-load switch was added to the circularly polarized ( $V$ ) system.

The approach finally used for the overall 5 GHz polarization instrumentation had one distinct advantage. The portion of the instrumentation for measuring  $V$  and  $I$  (one dual circularly polarized antenna with comparison-feed switching for

measuring V and comparison-load switching for measuring I) is the same as the systems used by Mackenzie University and Instituto Geofisico del Peru to measure V and I at 7 and 9.4 GHz. Even though the 5 to 9.4 GHz range is small, we have a consistent arrangement for systematic measurement of the circular polarization spectra of solar bursts over that range.

## 2. SPECTRA AND POLARIZATION OF MICROWAVE BURSTS

### 2.1 Spectra of cm- $\lambda$ Bursts

Unlike the studies of meter- $\lambda$  solar bursts, in which the morphological considerations (types I to V) are considered to have the greatest significance, AFGL's study of cm- $\lambda$  bursts has emphasized the spectrum (flux density vs frequency) of the radiation. Studies have been made of the time-varying spectrum during large bursts and statistically of the peak spectra of large numbers of mostly small bursts. The purpose has been to determine emission mechanisms and burst-region parameters such as magnetic field strength, electron density, and electron energy distribution.

An idealized peak flux density spectrum of a microwave burst (representative of actual burst spectra) is shown in Figure 1. It might be considered as having two components: the dm- $\lambda$  G type component (on the left in the figure) in which the flux density increases with decreasing frequency toward the meter- $\lambda$  range, and the cm- $\lambda$  C type component (on the right in the figure) for which the flux density reaches a single spectral maximum in the cm- $\lambda$  range. There are two other infrequently occurring types of cm- $\lambda$  spectra not shown in Figure 1. One is the A type, with flux density increasing with increasing frequency into the mm- $\lambda$  range (its flux density does not increase indefinitely; its spectral maximum is merely beyond the frequency coverage of the solar patrol). The other type, akin to the C type, has more than one (rarely more than two) spectral maxima within the cm- $\lambda$  range and is called miscellaneous or M type. Based on an analysis of more than 2400 bursts observed at Sagamore Hill over the 1968-1971 period, the percentage distribution of microwave bursts by spectral type is:

Pure G	19 percent
Pure C	54 percent
A	1 percent
Composite (GC)	21 percent
Miscellaneous (M)	5 percent. <sup>7</sup>

The significant finding is that the C type spectrum, either alone (pure C) or with a decimeter component added (GC), is present in about 75 percent of all microwave bursts.



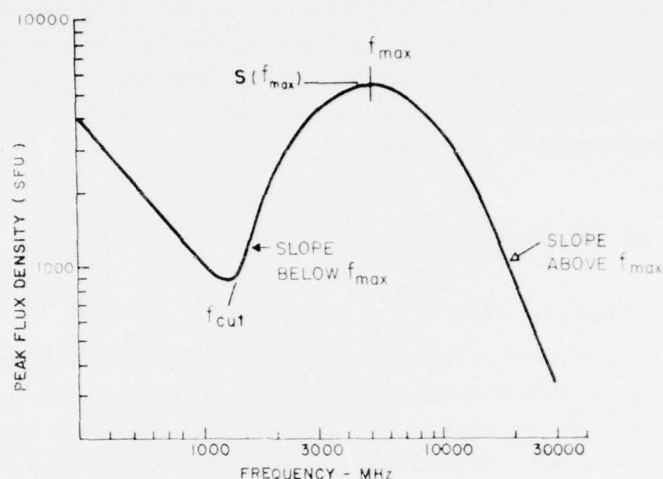


Figure 1. Idealized Peak Flux Density Spectrum of a Radio Burst (representative of actual burst spectra) Used for Spectral Classification

An additional classification category for C type spectra is the band in which the radiation has its maximum flux density. The Sagamore Hill patrol frequencies are associated with certain radar bands: 1415 MHz with L band, 2695 MHz with S band, 4995 MHz with C band, 8800 MHz with X band, 15400 MHz with K band. When the largest peak-flux-density value of a burst is measured at one patrol frequency, the spectral maximum is said to occur in the corresponding radar band, although the actual spectral-maximum-frequency ( $f_{max}$ ) obviously does not coincide precisely with any patrol frequency. The percentage distribution of the spectral maximum band of a large number of bursts with C type spectra or spectral component observed at Sagamore Hill between 1968 and 1971 is given in Figure 2. The percentage distribution was similar from year to year. The actual number of bursts in a given year correlated well with the average 4995-MHz slowly varying component flux density (mean non-burst flux density minus the minimum-background level) for the same year.<sup>7</sup>

Besides the distributional studies of  $f_{max}$ , the Solar Radio Astronomy Section of AFGL has also carried out studies of the below- $f_{max}$  spectral cutoff and the slope of the spectrum above  $f_{max}$ . The purpose of the former was to attempt to determine which attenuating mechanisms (self-absorption, free-free absorption, gyroresonance absorption, or ionized-medium emissivity suppression) were responsible for shaping the below- $f_{max}$  spectra of cm- $\lambda$  bursts in general<sup>7</sup> or of

certain peculiar bursts that were precursors of later catastrophic solar events.<sup>10</sup> The purpose of the latter was to see if the burst spectrum above  $f_{\text{max}}$  could be used to determine the energy parameters (the range of electron energies and the slope  $\Gamma$  of the assumed power-law number vs energy relationship  $N(E) \propto E^{-\Gamma}$ ) of the electrons producing the observed gyro-synchrotron emission. Ko has derived the proper emissivity formulas for theoretically calculating the intensity spectrum (emissivity vs frequency in units of gyrofrequency) at different observation angles for various power-law energy distributions ( $\Gamma = 2, 3, 4$ , etc.) over certain limited energy ranges, and carried out computerized calculations to obtain theoretical spectra.<sup>11</sup> An example of such theoretically computed microwave-burst spectra is shown in Figure 3.

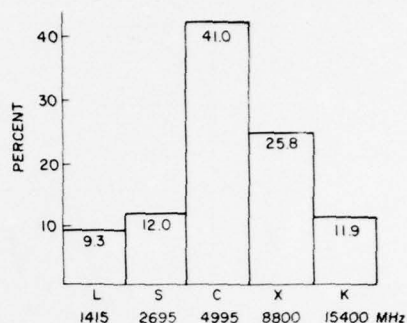


Figure 2. Percentage Distribution of the Observed Spectral Maxima of Bursts With C Type Spectra (Sagamore Hill data, 1968-1971). L, S, C, X, and K refer to the radar-band ranges where spectral maxima occurred

## 2.2 Polarization of cm- $\lambda$ Bursts

Solar burst radiation at centimeter wavelengths is produced by gyrosynchrotron emission from energetic (barely to mildly relativistic) electrons being braked (decelerated) by the strong burst-region magnetic field. (It is often called magnetobremssstrahlung – magnetic braking radiation.) Gyrosynchrotron emission is in general elliptically polarized, with the kind of polarization (from circular at one extreme to linear at the other) depending on the energy of the electrons and the direction of propagation relative to the magnetic field. (Radiation from relativistic electrons – synchrotron emission – is linearly polarized and highly directional.)

For gyrosynchrotron emission in a dense magnetoplasma, we must discuss propagation in terms of ordinary and extraordinary modes. Using quasi-longitudinal (QL) approximations (corresponding the conditions where the cm- $\lambda$  emission is generated), magneto-ionic theory shows that the ordinary and extraordinary

10. Castelli, J. P., Guidice, D. A., Forrest, D. J., and Babcock, R. R. (1974) Solar bursts at  $\lambda = 2$  cm on July 31, 1972, *J. Geophys. Res.*, 79:889.

11. Ko, H. C., and Chuang, C. W. (1976) Influence of the Solar Electron Energy Distribution on the Microwave Spectrum of Gyro-synchrotron Radiation, Ohio State University, AFGL-TR-76-0030.



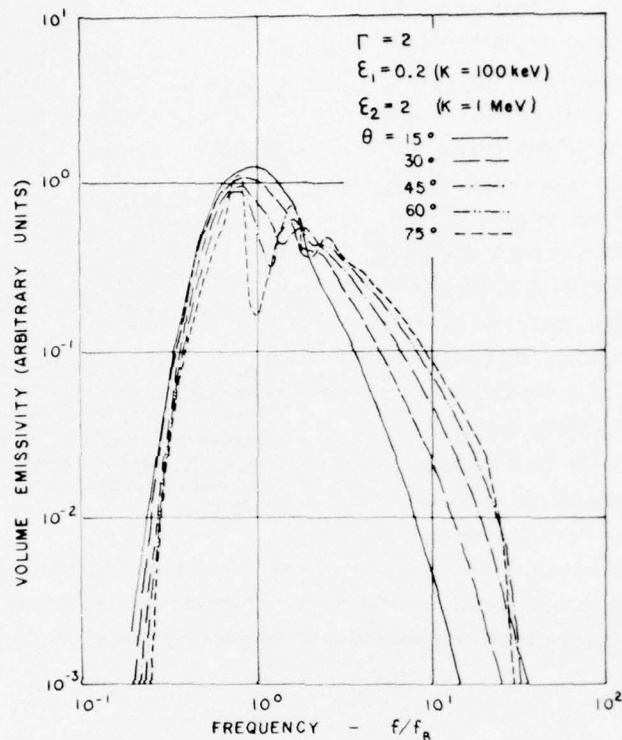


Figure 3. Radiated Power Spectra (theoretically computed) at Various Observation Angles  $\theta$  for a Group of Energetic Electrons Having a Power-Law Energy Distribution With  $\Gamma = 2$  and an Energy Range of 100 to 1000 keV

modes are circularly polarized for nearly all observation angles (angles between propagation direction and the magnetic field). The strong and variable spatial Faraday rotation effect within the emission source (the effect depends on electron density and magnetic field strength) destroys the coherence between ordinary and extraordinary modes and thereby eliminates the linear polarization.<sup>†</sup> Other effects (gyroresonant absorption, for example) attenuate the radiation, especially the

<sup>†</sup>In free space, an elliptically polarized wave can be analyzed into two coherent circularly polarized waves with opposite senses of rotation (of equal amplitude if the initial polarization is linear). If both waves were undisturbed by the propagation medium, they could be synthesized back to an elliptically polarized wave of the same axial ratio as the initial wave (to a linearly polarized wave if the initial polarization was linear).

ordinary-mode radiation. Takakura showed that the radiation from a solar cm- $\lambda$  burst is mainly emitted in the extraordinary mode.<sup>12</sup>

It is possible that further propagation (through the corona) might reintroduce some degree of linear polarization due to mode coupling effects as the circularly polarized extraordinary mode radiation crosses a quasi-transverse (QT) region in which the angle between the propagation path and the magnetic field is changing so that the direction of the longitudinal magnetic-field component reverses in the QT-region. The magnetic field "inhomogeneity" causes a partial coherent transformation of the extraordinary-mode radiation into ordinary-mode radiation. Combination (synthesis) of the two coherent modes after their propagation through the QT-region would then produce a linear component in the burst radiation propagating from the corona toward earth, even though any original linear polarization from the burst-region had been destroyed.

For the initially polarized ( $p_i$ ) portion of the burst radiation passing through the QT-region, Zheleznyakov<sup>13</sup> gives the resultant degrees of circular and linear polarization in terms of a characteristic parameter  $2\delta_0$  of the transformation region:

$$\begin{aligned}(p_c)_t &= -1 + 2e^{-2\delta_0} \\ (p_l)_t &= 2e^{-\delta_0} \sqrt{1 - e^{-2\delta_0}} \\ 2\delta_0 &= 10^{17} N_e B^3 / f^4 |da/dz| ,\end{aligned}$$

where  $N_e$  is the electron density ( $\text{cm}^{-3}$ ),  $B$  is the magnetic field (Gauss), and  $da/dz$  is the gradient of the observation angle in the QT region. The initially unpolarized portion,  $1 - p_i$ , of the burst radiation remains unchanged.

The mode-coupling-induced circular polarization goes to zero and the linear polarization (of the initially polarized part) goes to unity at  $2\delta_0 = \ln 2 = 0.69$ . This occurs at a transformation frequency ( $f = f_t$ ) given by

$$f_t \approx (1.4 \times 10^{17} N_e B^3 / |da/dz|)^{1/4} .$$

Figure 4 shows the circular and linear polarization as a function of frequency ( $f/f_t$ ) for (A) initially fully polarized radiation entering the QT-region and (B) for a more typical case of 25 percent initially polarized radiation. The abscissa of

12. Takakura, T. (1967) Theory of solar bursts, *Solar Phys.*, 1:304.

13. Zheleznyakov, V. V. (1970) *Radio Emission of the Sun and Planets*, Pergamon Press, Oxford, pp. 363-365.

Figure 4 is a log scale. We note that  $p_c = (p_c)_t p_i$  and  $p_f = (p_f)_t p_i$  and  $p = \sqrt{p_c^2 + p_f^2} = p_i$ . The mode-coupling effect, although it alters  $p_c$  and  $p_f$ , has no effect on the magnitude of the total degree of polarization  $p$ .

The obvious observational characteristic in this QT-region mode-coupling process is the change of the sense of polarization with frequency and the occurrence of the greatest linear polarization at the frequency of reversal. The change of the sense of circular polarization can also be explained by the effects of gyroresonance absorption; without any production of linear polarization. Linear polarization (if it is not destroyed by further Faraday-rotation effects in the corona) near the frequency of circular polarization reversal (minimum  $p_c$ ) would be important evidence of QT-region mode coupling. However, the failure to observe linear polarization does not necessarily rule out QT-region mode coupling, because of the various possible dispersal effects that could preclude seeing the linear polarization provided by mode coupling.

Akabane was the first (and only) observer to measure a linear polarization component in solar microwave bursts.<sup>14</sup> He found 25 out of 120 microwave bursts with flux densities greater than 100 solar flux units (sfu or  $10^{-22} \text{ W m}^{-2} \text{ Hz}^{-1}$ ) to have some small linear component. However, he did not calibrate the polarization characteristics of the antenna used for observations, and it cannot be ruled out that the linear polarization apparently observed was simulated by the antenna. Magun and Matzler measured the Stokes parameters of polarization at 8.9 GHz and found in 68 bursts observed no linear polarization within the accuracy limits (1 to 3 percent, depending on bandwidth) of their polarimeter.<sup>15</sup>

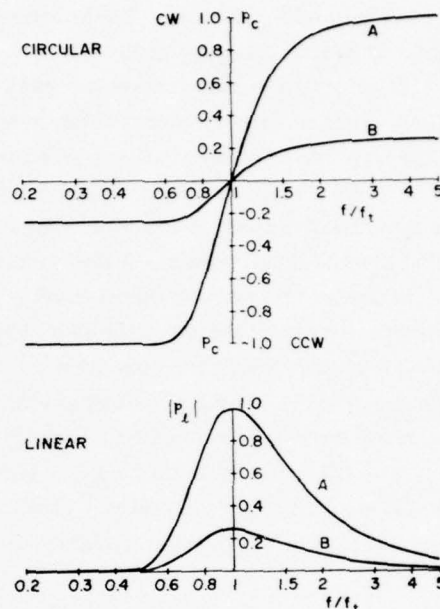


Figure 4. Theoretical Curves of Circular and Linear Polarization Resulting From Mode-Coupling Transformation in the QT-Region Above a Solar Burst. Shown are results for (A) fully polarized and (B) partially polarized ( $p_i = 0.25$ ) initial polarization

14. Akabane, K. (1958) On elliptical polarization of solar radio outbursts at 9500 MHz, *Publ. Astron. Soc. Japan*, 10:99.

15. Magun, A., and Matzler, C. (1973) On the observation of solar microwave bursts, *Solar Phys.*, 30:489.

### 3. WHOLE-SUN $\text{cm-}\lambda$ POLARIZATION MEASUREMENTS

#### 3.1 Circular-Polarization Instrumentation at 9.4 and 7 GHz

The instrumentation used at Huancayo Observatory (9.4 GHz) and Itapetinga Observatory (7.0 GHz) to measure the circular polarization and total intensity (Stokes parameters V and I) of solar microwave emission is quite similar in concept, differing only in the details and components of the various radiometer sections. The general principles of a dual-modulated radiometric system will be presented here. The equipment used in the 9.4 GHz system will be shown; techniques used for the measurements at 7 GHz are similar and will not be described in this report.

An antenna with dual (right and left) circular polarization capabilities receives the incident solar-radiated microwave power. The antenna's beamwidth is several times that of the sun so that the antenna's response is relatively independent of the emission's origin (location) on the solar disk. The power received by the right circularly polarized receptor element and the power received by the left circularly polarized receptor element come down separate paths (waveguides) to the input ports of a modulator switch that alternately connects each path to the remainder of the radiometric system. A constant audio-frequency (typically 70 to 1000 Hz) switch rate with a 50 percent duty cycle is used. This is often called the comparison-feed mode of operation.

Next in the radiometer chain is another modulator switch. This one alternately connects the output from the comparison-feed switch and the output from a matched load (often temperature stabilized) to the first stage of the receiver network. This switching between the antenna input and a matched load is often called the comparison-load mode of operation or Dicke switching. The switching rate of the comparison-load switch is at another audio frequency far away from (and not harmonically related to) the switching rate of the comparison-feed switch. The oscillators driving the two switches are independent.

The output from the second modulator switch goes to a mixer that converts from the incident microwave frequency (that is, 9.4 or 7 GHz) to an intermediate frequency (typically 30 or 60 MHz). The i.f. signal is amplified by a preamplifier (usually a part of the mixer package) and then by a main i.f. amplifier. This is followed by a diode detector that detects the audio-frequency modulation on the i.f. signal. The detected signal is then fed to each of two synchronous (that is, phase-sensitive) detectors. One is synchronized to the modulation sent to the comparison-feed switch, and the other to that sent to the comparison-load switch.



One synchronous detector produces a d-c voltage (a rectified sine wave later smoothed to slowly changing dc) correlated with the changing input to the comparison-feed switch. This voltage is proportional to the difference between the powers received by the right-circular-sensitive and the left-circular-sensitive receptors of the antenna. It measures the Stokes parameter V.

The other synchronous detector produces a d-c voltage correlated with the changing input of the comparison-load switch. This voltage is proportional to the difference between the power from the antenna line and the constant power of the matched load. It measures the average power of the antenna line — that is, one-half the sum of the powers received by the right-circular and left-circular receptors of the antenna. This is a measure of the total power of the incident solar emission — that is, the Stokes parameter I.

The outputs from the two synchronous (phase-sensitive) detectors are integrated (smoothed) and further amplified to a level suitable for driving the pens on analog pen-recorders to give time profiles (flux density vs time) of V and I. Calibration of the pen-recorder signals in terms of antenna temperature ( $T_A$ ) is achieved by the introduction of known temperature differences on the antenna lines; for example, the physical temperature of a matched load measured by a thermometer or calibrated thermistor and the near-zero temperature of the "cold" sky at microwave frequencies. Another  $T_A$  calibration technique employs a standard noise source (for example, an argon noise tube across a waveguide section) to produce the noise equivalent of a constant temperature.

Measurements of V and I in terms of flux density (the desired result) is achieved through the determination of the antenna effective area  $A_e$  in the expression  $S = 2kT_A/A_e$  where S is flux density and k is Boltzmann's constant. Effective area can be determined by comparison of the response of the antenna used for the polarization measurements with the response of a standard gain horn (whose gain or effective area can be calculated from its physical dimensions), or (using only the polarization antenna) by comparison of the solar emission response to the response from other radio sources whose flux densities are known. Such techniques have been described by Guidice and Castelli.<sup>16, 17, 18</sup>

16. Guidice, D.A., and Castelli, J.P. (1968) The Determination of Antenna Parameters by the Use of Extraterrestrial Radio Sources, Air Force Cambridge Research Laboratories, AFCRL-68-0231.
17. Guidice, D.A., and Castelli, J.P. (1971) The use of extraterrestrial radio sources in the measurement of antenna parameters, IEEE Trans. Aerospace and Elec. Sys., AES-7:226.
18. Castelli, J.P., and Guidice, D.A. (1975) Verification of solar patrol calibration at 15.4 GHz, Astrophys. Let., 16:71.

A block diagram of the 9.4 GHz Huancayo solar polarization instrumentation is given in Figure 5. Matched absorbers (capable of being inserted into the "right-circular" and "left-circular" waveguide runs from the antenna) are used for calibration of the polarized solar emission (V), while a noise source is utilized for calibration of the total intensity I. An 80 Hz oscillator is used to drive the comparison-feed (polarization-selector) switch, and a separate 220 Hz oscillator is used to drive the comparison-load (Dicke modulator) switch. A phase-locked klystron is used to supply the local oscillator signal to the balanced mixer.

Figure 6 shows the 3-ft parabolic antenna of the equatorially mounted solar tracker used for the 9.4 GHz measurements at the Huancayo Observatory. The electronic components in the radiometer "front end" (from the i. f. preamplifier leftward in the block diagram, Figure 5) are in the instrument box in back of the antenna. Figure 7 shows the radiometer "back end" components in the receiver building at the Huancayo Observatory. Figure 8 shows the parabolic antenna and equatorially mounted tracker used for the 7 GHz polarization measurements at the Itapetinga Observatory. Figure 9 shows the radiometer "back-end" components in the receiver building at the Itapetinga Observatory.

### 3.2 Sagamore Hill 5 GHz Polarization Instrumentation

The whole-sun 5 GHz solar polarization instrumentation at the Sagamore Hill Radio Observatory measures the Stokes parameters of polarization directly. All measurements are of differences or sums of powers received at orthogonal polarizations. There are no techniques involving multiplication or correlation of voltages; therefore, there are no electronic-processing complexities or large errors due to cross-polarized responses (crosstalk).

A block diagram of the Sagamore Hill instrumentation is given in Figure 10. Three 6-ft-diam parabolic antennas are installed on an equatorially configured MP-61 mount that turns in hour angle at solar rate to keep the beams pointed at the center of the sun. The beamwidth of each antenna is about  $2.5^\circ$ .

Single sideband operation of the radiometric networks is achieved through the use of a 50-MHz-bandwidth r-f filter in each network just before its balanced mixer. Except for a common Gunn-effect oscillator supplying local oscillator power to the mixers, the V/I, Q, and U networks are electronically independent. The equipment to the left of the dashed line in the block diagram is housed in a common instrument box (for shelter purposes) on the mount in back of the three antennas. The Q and U networks are exactly similar electronically; the only difference between them is the orientation of the response of their dual linearly polarized antennas: the Q antenna is oriented  $0^\circ/90^\circ$  (that is, horizontal/vertical) while the U antenna is oriented  $45^\circ/135^\circ$ . The overall linear polarization  $p_l$  is measured by  $\sqrt{Q^2 + U^2}/I$ .



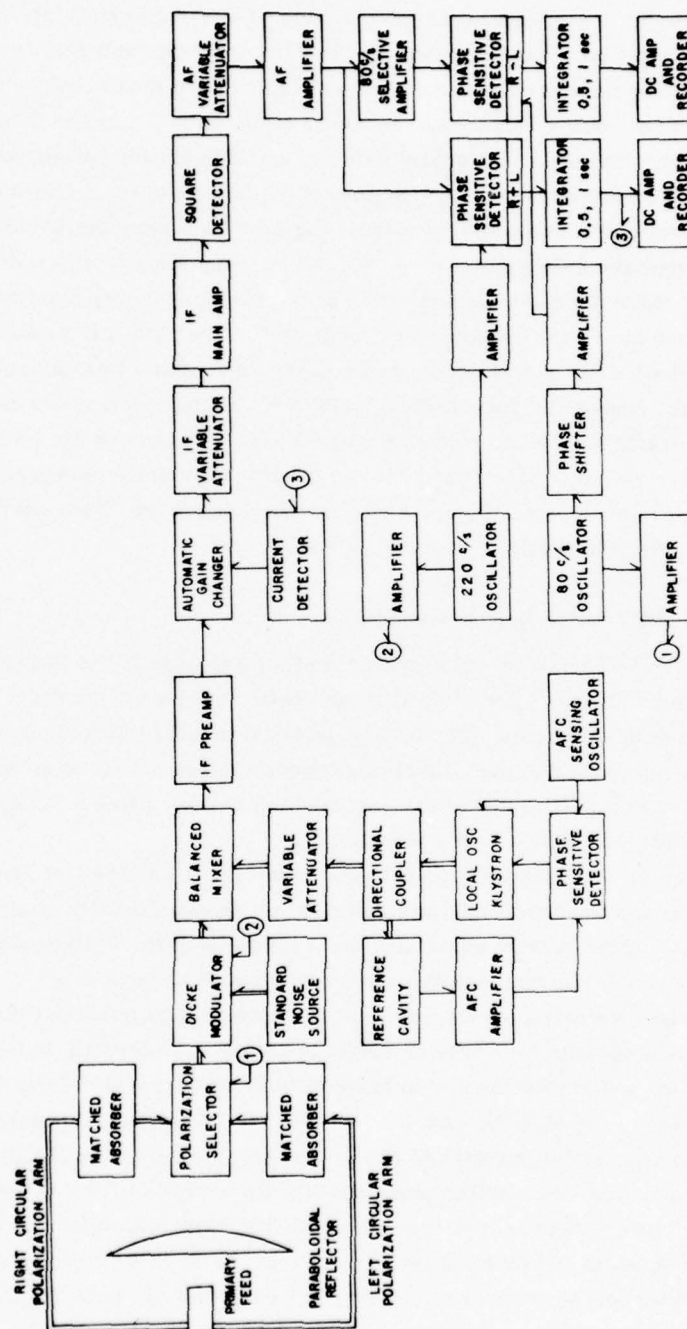


Figure 5. Block Diagram of the Instrumentation Used at the Huancayo Observatory to Measure the Circular Polarization and Total Intensity of Solar Emission at 9.4 GHz

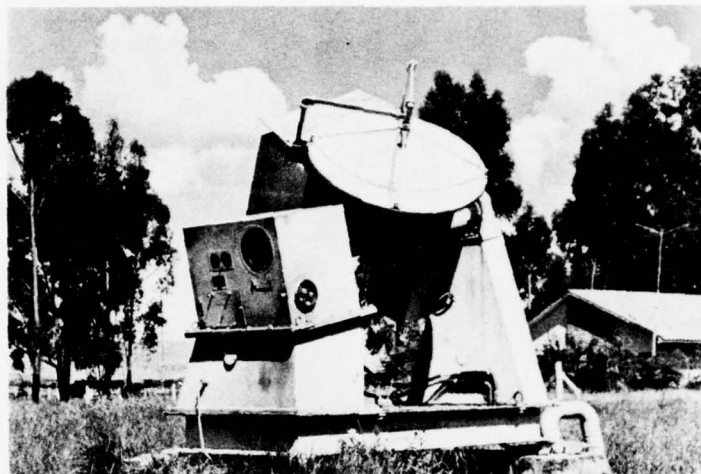


Figure 6. Antenna and Equatorially Mounted Tracker Used for 9.4 GHz Solar Polarization Observations at Huancayo Observatory

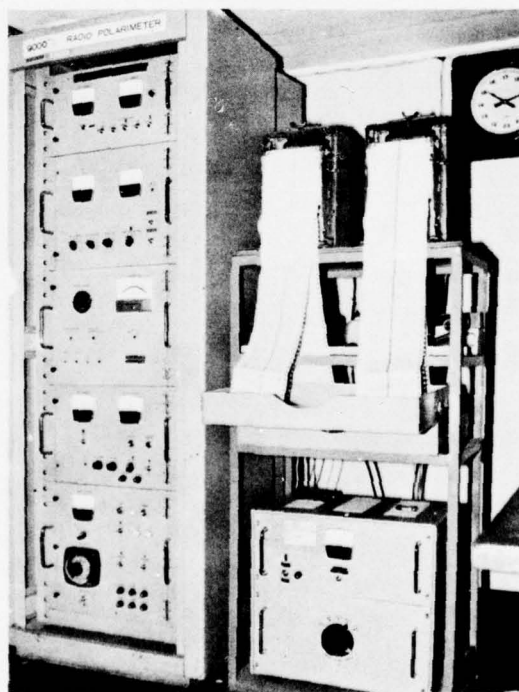


Figure 7. Radiometer "Back End" Components in the Receiver Building at the Huancayo Observatory

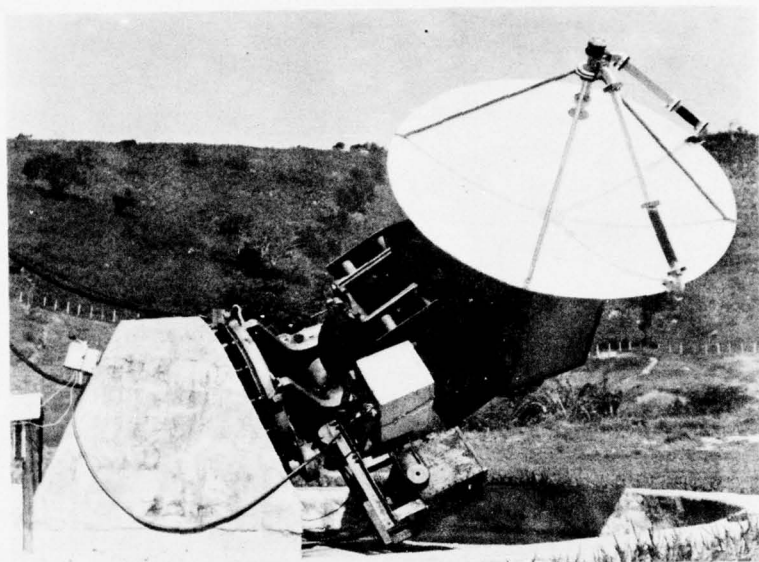


Figure 8. Antenna and Equatorially Mounted Tracker Used for 7 GHz Solar Polarization Observations at Itapetinga Observatory

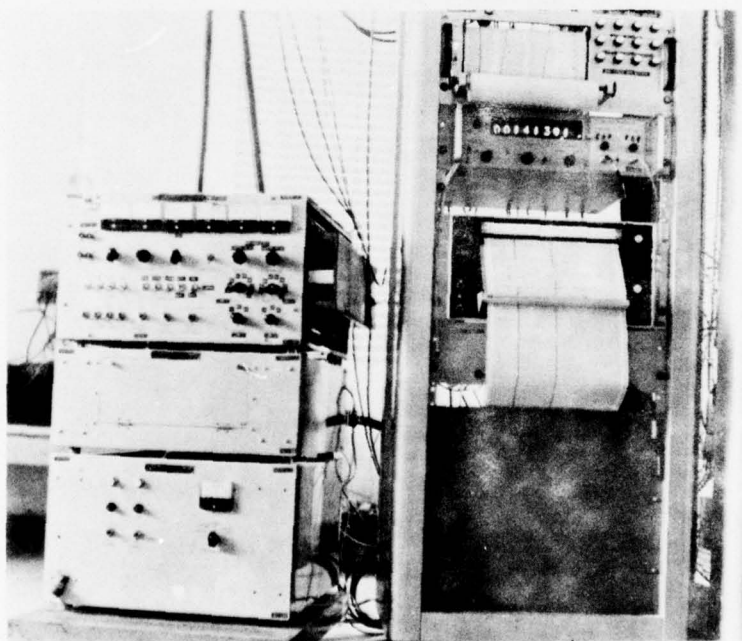


Figure 9. Radiometer "Back End" Components in the Receiver Building at the Itapetinga Observatory

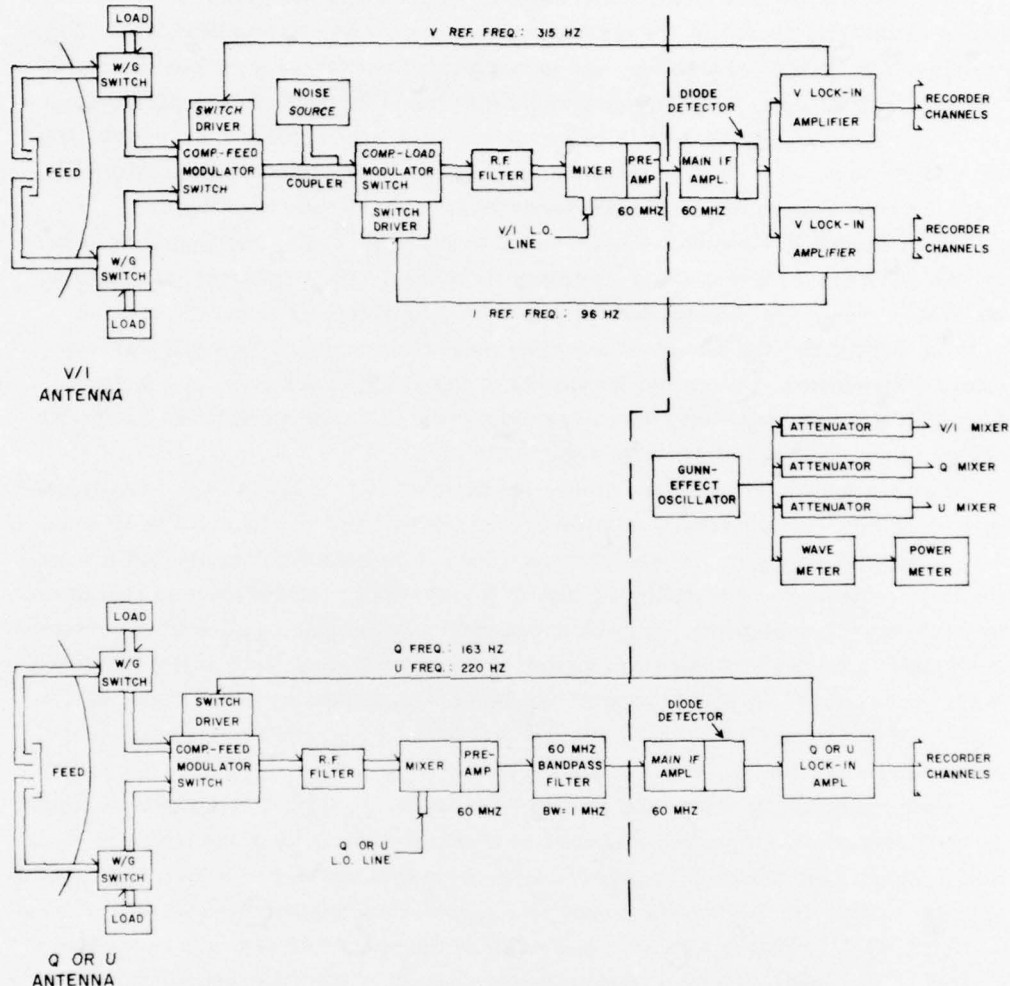


Figure 10. Block Diagram of the Sagamore Hill 5 GHz Radiometric Instrumentation Capable of Measuring the Four Stokes Parameters of Polarization

The V/I network operates with both a comparison-feed switching mode (to measure V) and a comparison-load switching mode (to measure I). The Q and U networks each operate with only a comparison-feed switching mode. This property gives the Q and U networks a factor of two sensitivity advantage over the V/I network in this regard. The reference generator for driving each modulator switch is located in the lock-in amplifier responsible for detecting the modulation put on the radiometric signal by that switch. The lock-in amplifier combines the functions



of reference generation, audio (reference-frequency) amplification, synchronous (phase-sensitive) detection, integration (smoothing), and d-c amplification. Widely separated reference frequencies, not harmonically related, are employed to prevent any interactions in the signal-processing chains for each Stokes parameter.

The radiometer bandwidth is determined by the bandwidth of the i. f. (60 MHz) amplifier chain. For the V/I network, the bandwidth is about 16 MHz, resulting from the combination of the 20 MHz bandwidths of the preamp and the main i. f. amplifier (both tube-type with double-tuned circuitry).<sup>19</sup> For the Q and the U networks, the bandwidth is 1 MHz, resulting from the 1 MHz bandwidth i. f. filter installed between the preamp and the main i. f. amplifier. The narrower bandwidth is needed for the linear polarization measuring networks to limit Faraday-rotation dispersion. The wider bandwidth of the V/I network gives it a factor of four (that is,  $\sqrt{16}$ ) sensitivity advantage over the Q and U network in the bandwidth aspect of the minimum detectable signal relation.

Calibration of the polarized Stokes parameters (V, Q and U) is accomplished by recording the temperature difference between the cold sky (about 5 to 10 K at 5 GHz, depending mainly on weather conditions – the galactic contribution is small for this frequency) and a stabilized matched load (whose temperature is measured by calibrated thermistors). An electromechanical waveguide switch in each waveguide path from the feed allows selection of the antenna line (cold sky) or matched load. Note that V, Q, and U have an algebraic sign indicative of the sense of polarization; the "ambient load/cold sky" calibration is therefore made in each (algebraic) direction on the recorder scale.

Calibration of the Stokes parameter I (no algebraic sign, I is always positive) can be accomplished by recording the temperature difference of the matched loads or by using a calibrated noise generator (coupled into the line as shown in Figure 9) above cold sky. In the former technique (customarily employed), both polarization paths in the V/I network are first connected to the feed (cold sky) and then both to their matched loads (whose temperatures are noted). The difference between the average load temperature and the cold sky temperature is recorded for calibration.

Figure 11 shows the three parabolic antennas and solar tracker used for the Sagamore Hill 5 GHz polarization observations. The radiometer "front end" equipment is housed in the instrument box in back of the antennas. The radiometer "back end" equipment (main i. f. amplifiers, lock-in amplifiers, recorders, etc.) are inside a trailer located about 20 ft north of the solar-tracker pad. A view of the electronics inside the trailer is shown in Figure 12.

19. Seely, S. (1950) Electron Tube Circuits, McGraw-Hill, New York, p. 206.

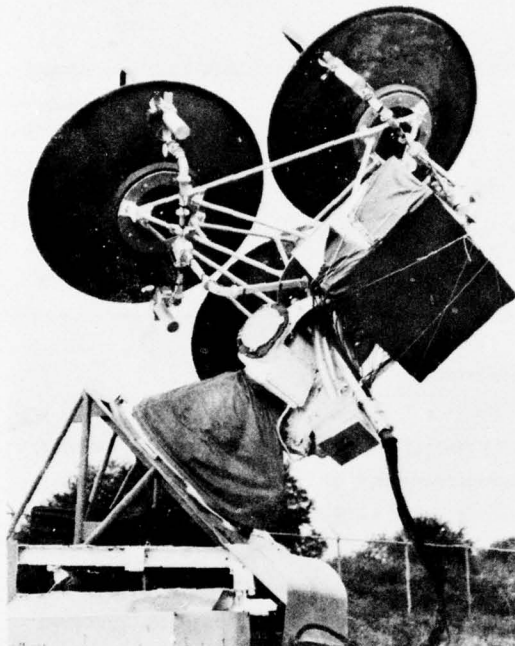


Figure 11. Three Antennas and Instrument Box on Equatorially Mounted Solar Tracker Used for 5 GHz Solar Polarization Observations at the Sagamore Hill Radio Observatory

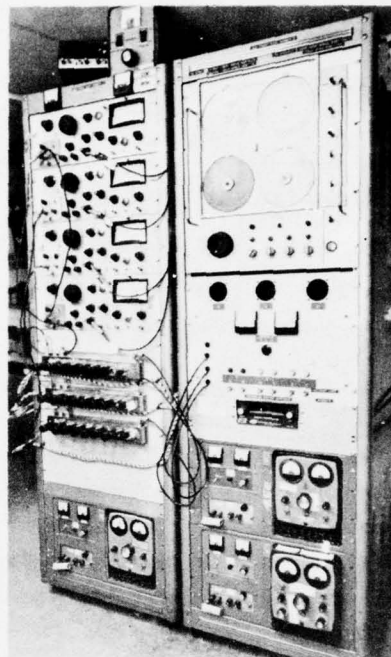


Figure 12. Tracker Control Panel and Radiometer "Back End" Components Housed in a Trailer Used for 5 GHz Polarization Observations at Sagamore Hill. Analog recording equipment (not shown) is installed in another rack

#### 4. RESULTS OF POLARIZATION SPECTRA OBSERVATIONS

##### 4.1 Polarization-Patrol Burst Survey

Since the approach used for the 5 GHz Stokes parameter measurements at Sagamore Hill resulted in a system that determines circular polarization and total intensity (flux density) in the same way as the 7 GHz and 9.4 GHz systems at Itapetinga and Huancayo, a limited study of the circular polarization spectra of radio bursts over the frequency range covered by these stations was undertaken. Table 1 lists some parameters for the three stations.



Table 1. Geographic and Instrumentation Parameters of Polarization-Study Stations

Station	Latitude	Longitude	Center Freq.	Wave-length	Reception*	Beam-width
Sagamore Hill	43°38'N	70°49'W	4965 MHz	6.0 cm	SSB	2.5°
Itapetinga	23°11'S	46°43'W	7000 MHz	4.3 cm	DSB	2.7°
Huancayo	12°19'S	75°19'W	9400 MHz	3.2 cm	DSB	2.6°

\*SSB = single sideband; DSB = double sideband

In any statistical investigation of the properties of large numbers of bursts, one must specify a consistent time of measurement within each burst to obtain meaningful results. The moment typically chosen is the time of the greatest radiation; for example, peak flux density. As in previous investigations of the spectral parameters of large numbers of bursts by AFGL's Solar Radio Section,<sup>7</sup> the "peak flux density" approach was employed in the circular polarization spectral studies described in this report.

The survey period of the bursts used in the polarization studies is August 1972 to December 1973. Since the 9.4 and 7 GHz whole-sun polarization observations were carried out from long before to long after this period, the limitation is due to the 5 GHz observations. Routine operation of the 5 GHz polarization system began in August 1972; this marks the beginning of the spectral study period. The ending of the period in December 1973 was caused to some extent by the lack of full-availability of personnel to operate the 5 GHz system, but mainly by the lack of burst activity on the sun in 1974.

In general, the Sagamore Hill polarization observations were made only on weekdays from about 0800 to 1600 local time. The observations from the other two stations were for the most part daily sunrise-to-sunset patrols. To obtain "spectral" information, one needs, as a minimum, data from the patrols at the ends of the 5 to 9.4 GHz frequency range. Since the 5 GHz operation imposed the limit on observing bursts, the polarization spectra survey was conducted by taking all the bursts observed by the 5 GHz system in the August 1972 to December 1973 period and then looking for corresponding burst occurrences in the burst data submitted to AFGL by Instituto Geofisico del Peru and Mackenzie University under their AFOSR grants.

To be included in the survey, a burst was required to be observed in flux density (total intensity I) at 5 GHz and 9.4 GHz. To eliminate unreliable observations of very small bursts, it was also required that a burst have a peak flux density of at least 5 sfu (solar flux units =  $10^{-22} \text{ W m}^{-2} \text{ Hz}^{-1}$ ) at one of the three polarization patrol frequencies.

In the August 1972 to December 1973 period, about 90 solar bursts of possible use in the polarization spectral study were measured by the Sagamore Hill 5 GHz polarization instrumentation. For about 45 of these bursts, corresponding emission data at 9.4 GHz were obtained from Instituto Geofisico del Peru (Huancayo); for about 35 bursts, corresponding data at 7 GHz were obtained from Mackenzie University (Itapetinga).

The relatively low correlation of the 9.4 and 7 GHz burst data with the Sagamore Hill results occurs for several reasons. The main reason is that the polarization observations were made at three separate observatories (in contrast to the 245 to 35000 MHz flux density observations all made at Sagamore Hill); hence, there is no reinforcement of measurements. Many low-level bursts seen alone (particularly small gradual rise and fall type or interference-like impulsive bursts) are simply not taken as bursts and reported. For the polarization survey we had only the reported burst data from Instituto Geofisico del Peru and Mackenzie University, not the analog records from Huancayo and Itapetinga. Another reason for the lack of corresponding observed bursts is the actual spectra of the bursts. Some bursts have a fully measurable peak flux density at one frequency and only a marginal or below-detection peak flux density at another frequency.

Regarding the fewer burst correlations in the Mackenzie records (compared to I. G. del Peru), the obvious explanation is the better longitudinal overlap of Huancayo with Sagamore Hill. Itapetinga is roughly  $24^\circ$  east of Sagamore Hill, while Huancayo is only  $4.5^\circ$  west of Sagamore Hill. In addition, several of Itapetinga's "off the air" periods happened to occur when Sagamore Hill was observing bursts at 5 GHz.

Overall, it must be noted that in the survey period both the 9.4 GHz and the 7 GHz polarization systems observed many more bursts than Sagamore Hill's 5 GHz system, mainly because of the manpower-limited observing times imposed on the 5 GHz polarization-system operations.

The pertinent emission data for the 45 bursts used in the polarization spectra study are presented in Table 2. Bursts are numbered (in chronological order) for later convenience in referring to them. The burst start times and peak times listed represent the best compromise of the data from the three patrols; no significant timing problems arose. The morphological type for each burst (from its flux density vs time profiles) was designated as either impulsive (IMP), complex (CPX), or gradual rise and fall (GRF). The spectral classification was obtained

Table 2. Parameters of Bursts Used in Polarization Spectra Study

Burst No.	Date	Times (UT) Start Peak	Morph. Type	Spectrum Class.	5 GHz Observ.			7 GHz Observ.			9.4 GHz Observ.			Remarks
					I sfu	V sfu	p <sub>c</sub> %	I sfu	V sfu	p <sub>c</sub> %	I sfu	V sfu	p <sub>c</sub> %	
1972														
1	22 Aug	1210.0	GRF	C2L	20.0	0	0	33.0	1.0	3 L	29.6	0	0	Essentially unpolarized.
2	23 Aug	1911.0	IMP	C2C	102.0	5.0	5 L	Not operating			90.5	17.7	20 R	Pol. reversal (est. ~6 GHz); est. spectral max. about 6 GHz.
3	28 Aug	1633.6	IMP	C1X	19.2	0	0	31.8	1.6	5 L	53.9	0	0	Essentially unpolarized.
4	30 Aug	1700.0	IMP	M2	55.0	10.0	18 L	31.8	7.0	22 L	26.1	6.5	25 L	
5	5 Sept	1555.0	GRF	C1C	6.7	0	0	Not reported			9.3	0	0	Unpolarized.
6	5 Sept	1725.0	GRF	C1C	7.5	2.0	27 R?	Not reported			4.7	0	0	Low-level burst, possibly unpolarized.
7	24 Oct	1246.1	GRF	C1C	31.9	7.2	23 R	43.4	6.9	16 R	33.3	6.4	19 R	
8	24 Oct	1342.0	IMP	G2C1K	7.2	0	0	Not reported			38.8	5.4	14 R	Flux den. & pol. increasing with incr. freq.
9	24 Oct	1800.2	IMP	G1C2X	46.0	5.9	13 R	85.5	17.6	21 R	114.6	30.0	26 R	Flux den. & pol. increasing with incr. freq.
10	24 Oct	1832.0	GRF	G1C1X	9.8	2.0	20 L	Not reported			25.9	5.9	23 R	Pol. reversal (est. ~7 GHz); est. spectral max about 7-8 GHz.
11	27 Oct	1842.4	CPX	G1C1C	21.1	1.5	6 L	Not reported			29.8	2.4	8 R	Pol. reversal (est. ~7 GHz); est. spectral max about 6-7 GHz.
12	27 Oct	1936.5	IMP	C2C	108.0	13.9	13 R	Not operating			96.8	26.6	27 R	
13	30 Oct	1446.1	IMP	C1C	34.3	10.8	30 L	47.1	0	0	16.9	5.9	35 R	Pol. reversal (est. ~7 GHz); est. spectral max about 6-7 GHz.
14	30 Oct	1641.6	CPX	C2X	151.	20.7	14 L	162.2	7.1	4 L	62.0	8.4	14 R	Pol. reversal (est. ~8 GHz); est. spectral max about 7-8 GHz.
15	30 Oct	1734.8	IMP	G2C2X	50.3	~0	0	54.4	8.4	15 R	65.8	32.6	50 R	Flux den. & pol. increasing with incr. freq.
16	1 Nov	1401.0	IMP	Not avail.	11.6	2.8	24 L	Not reported			11.4	7.1	62 L	
1973														
17	11 Jan	1756.0	CPX	G3C2K	91.0	3.4	4 R	227.0	0	0	409.0	5.7	1 R	Very low circ. pol.; 2% apparent linear pol. observed at 5 GHz.
18	6 Mar	1950.0	IMP	G2C1C	14.0	0	0	10.8	0.6	6 R?	20.6	0	0	Possibly unpolarized.
19	3 Apr	1852.6	IMP	C1C	25.5	2.8	11 R	Not operating			14.2	-	<2 R	Flux den. & pol. increasing with decr. freq.
20	4 Apr	1838.1	IMP	G1C1X	6.2	3.7	60 L	Not reported			19.8	5.5	28 R	Pol. reversal (est. ~8 GHz); est. spectral max about 8-9 GHz.
21	9 Apr	1542.4	IMP	G3C2L	44.1	4.6	10 R	37.5	2.8	7 R	25.7	5.3	20 R	
22	9 Apr	1745.4	IMP	G3C2L	19.6	4.7	24 R	25.2	3.5	14 R	25.7	5.3	20 R	
23	10 Apr	1908.1	CPX	G2C2X	104.0	18.9	18 L	173.0	23.7	14 L	105.0	24.2	23 L	Apparent 4% linear pol. observed at 5 GHz.
24	11 Apr	1404.6	IMP	C2C	89.1	16.4	18 L	~80.0	4.2	5 L	66.9	0	0	Flux den. & pol. increasing with decr. freq.
25	11 Apr	1620.7	CPX	C2L	43.3	5.5	13 R	75.3	11.4	15 R	48.3	11.0	23 R	

Table 2. Parameters of Bursts Used in Polarization Spectra Study (Cont.)

Burst No.	Date	Times (UT) Start Peak	Morph. Type	Spectrum Class.	5 GHz Observ. I V P <sub>c</sub> sfu sfu % s	7 GHz Observ. I V P <sub>c</sub> sfu sfu % s	9.4 GHz Observ. I V P <sub>c</sub> sfu sfu % s	Remarks
26	1973							
27	11 Apr	1842.4	CPX	M3	120.0 6.4 5 L	233.0 14.4 6 L	201.0 - <2 R	Very low circ. pol.
28	11 Apr	2033.8	GRF	GIC2L	64.5 9.2 14 L	Not operating	39.0 0 0	Flux & pol. increasing with decr. freq.
29	24 Apr	1412.5	IMP	G2C2C	320.0 172.0 54 L	215.0 74.5 35 L	172.0 91.1 53 L	Apparent 0% linear pol. observed at 5 GHz.
30	24 Apr	1927.2	CPX	G3C2S	65.2 24.0 37 L	46.1 15.7 34 L	27.2 8.9 32 L	Flux den. & pol. increasing with decr. freq.
31	26 Apr	1957.9	IMP	G2C1C	44.3 4.2 9 R	Not operating	27.6 11.9 43 L	Pol. reversal (est. ~6 GHz); est. spectral max about 3-6 GHz.
32	30 Apr	1729.0	IMP	C2K	4.8 0 0	38.2 0 0	71.6 - <2 R	Essentially unpolarized.
33	1 May	1319.2	IMP	G3C1S	30.8 6.6 22 R	20.8 3.0 14 R	20.4 - <2 R	Flux den. & pol. increasing with decr. freq. App. 8% linear pol. observed at 3 GHz.
34	1 May	1419.2	CPX	C2X	26.2 0 0	40.4 0 0	91.7 - <2 R	Essentially unpolarized.
35	1 May	1824.6	GRF	G2C1X	24.1 0 0	20.5 1.5 7 R?	27.2 - <2 R	Essentially unpolarized.
36	3 May	1552.6	IMP	G2C1X	8.1 0 0	16.7 1.2 7 R?	10.0 0 0	Essentially unpolarized.
37	17 May	1344.4	IMP	G2C1X	15.8 4.3 27 L	20.8 2.4 12 L	27.9 - <2 L	Essentially unpolarized.
38	17 May	1356.6	CPX	G2C2S	31.6 1.9 6 L	16.4 0 0	10.1 0 0	Essentially unpolarized.
39	17 May	1909.1	CPX	G3C7K	250.0 38.2 15 L	283.0 72.4 26 L	799.0 129.0 16 L	App. 4% linear pol. observed at 5 GHz.
40	29 June	1946.4	CPX	G2C2X	121. 6.4 5 R	180. 33.8 19 L	163. 36.2 22 L	At 1948.7, pol. reversal with freq. at ~6 GHz (spectral max. at ~7 GHz).
41	10 July	1355.4	IMP	C1K	9.1 1.9 21 R	23.5 5.2 22 R	20.2 0.6 3 R	At 1949.0, a pol. reversal with time at 5 GHz. App. 4% linear pol. at 5 GHz.
42	7 Aug	1845.1	CPX	G2C2L	21.0 2.5 12 R	Not reported	10.5 0 0	Flux den. & pol. increasing with decr. freq.
43	9 Aug	1414.6	IMP	M1	8.3 1.0 59 R	44.7 0 0	12.0 0.3 3 R	Flux den. & pol. increasing with decr. freq.
44	9 Aug	1550.6	CPX	G3C1L	20.3 6.1 30 R	Not reported	29.0 - <2 R	Flux den. & pol. increasing with decr. freq.
45	5 Sept	1828.3	IMP	G3C2C	55.8 17.9 30 L	28.3 4.2 15L	24.3 0.6 2 L	Flux den. & pol. increasing with decr. freq.
46	7 Sept	1155.0	CPX	G2C2C	304. 24.5 8 L	Not reported	239. 1.6 1 L	Flux den. & pol. increasing with decr. freq.

\* Circular polarization P<sub>c</sub> is given as a percentage. The L (for left) or R (for right) indicates the sense of P<sub>c</sub>.



from the peak flux density records of the regular Sagamore Hill solar radio patrol. The notation is based on the classification scheme of Guidice and Castelli described in Section 2.2 of this report. The numbers after the G, C, or M refer to the intensity levels of peak flux density: 1 for <50 sfu; 2 for 50-500 sfu, and 3 for >500 sfu.<sup>7, 20, 21</sup>

The middle groups of columns in Table 2 give the Stokes parameters I and V (in solar flux units) and the circular polarization  $p_c$  (as a percentage) for each polarization patrol frequency. The sense of circular polarization (L = left; R = right) is also given in the  $p_c$  columns. For the 7 GHz data, "not reported" indicates that Itapetinga was apparently operating but no data on the burst appeared in the monthly records supplied to AFGL (formerly AFCRL). The notation "not operating" shows that the burst occurred outside the indicated operating time of the patrol; this would include occurring beyond reliable viewing, for example, near or below the horizon. (There is no such notation in the 5 GHz or 9.4 GHz column groups, since data from these patrols constitute a necessary condition for inclusion of a burst in Table 2.)

#### 4.2 Results and Discussion

From the data of Table 2, some limited distributional results were obtained concerning the circular polarization spectra (at peak intensity) of solar microwave bursts in the 5 to 9.4 GHz frequency range:

1. The large majority of bursts are circularly polarized with varying polarization over the frequency range.
2. For most bursts where the circular polarization  $p_c$  increases toward the upper or lower end of the 5 to 9.4 GHz range, the total intensity I also increases in that direction.
3. The few bursts with circular-polarization sense reversal in the 5 to 9.4 GHz range also have a total intensity spectral maximum within the range.

For the bursts listed in Table 2, the occurrence of significant circular polarization at peak intensity was found to be 76 percent. In examinations of bursts from individual polarization patrols and over a wider survey period than that of Table 2, it was found that about 80 percent of bursts have significant circular polarization. Hence, the Table 2 results might be considered representative of more broadly based investigations.

20. Castelli, J. P., and Guidice, D. A. (1972) On the Classification, Distribution and Interpretation of Solar Microwave Burst Spectra and Related Topics, Air Force Cambridge Research Laboratories, AFCRL-72-0049.

21. Castelli, J. P., and Guidice, D. A. (1976) Impact of current solar radio patrol observations, Vistas in Astronomy, 19:355.

Of the 11 bursts of Table 2 without significant circular polarization, 4 were gradual rise and fall bursts (of the 6 GRF bursts in Table 2, 4 were unpolarized). Thus when the GRF bursts are excluded, the percentage of occurrence of significant circular polarization (for IMP and CPX bursts) is greater than 80 percent. Similar results are found in the broader-based surveys.

In regard to the second result, 11 bursts in Table 2 were found where both  $I$  and  $p_c$  clearly increased toward the 9.4 GHz or the 5 GHz end of the polarization-patrol range (in 3,  $I$  and  $p_c$  increased toward the upper end; in 8,  $I$  and  $p_c$  increased toward the lower end). The increases in  $I$  found in the polarization-patrol data were confirmed by indications from the spectral classification column; this column is based on observations independent of the polarization-patrol results, that is, from the regular Sagamore Hill flux density patrol. (The consistency of the polarization-patrol and Sagamore Hill data was a necessary condition for citing the 11 bursts in which the  $I$ - $p_c$  phenomenon was found.) As for the opposite situation within the 5 to 9.4 GHz range where  $I$  increased in one direction and  $p_c$  in the other, only three possible cases (bursts) could be found — even when the requirement of corroborating  $I$  data was set aside. There were also some cases of polarized bursts in which no particular trend in  $I$  or  $p_c$  toward the upper or lower end of the 5 to 9.4 GHz range could be found.

Because of the small frequency range and number of bursts, no grand-scale conclusions should be drawn here. A possible simple explanation of the  $I$ - $p_c$  correspondence phenomenon is that the part of the burst radiation that is highly circularly polarized also has a relatively narrow band of spectral emission. This explanation can be justified by noting that the theoretical emission for low-energy (non to barely relativistic) electrons is inherently highly circularly polarized and is concentrated in the lower harmonics with a very rapid drop-off (order of magnitude or more per harmonic) on the high-frequency side of the spectral maximum ( $f_{\max}$ ). Any of several absorption phenomena (see references 7 and 10) can cause a steep emission drop-off on the low-frequency side to go along with the above- $f_{\max}$  drop-off, giving an overall narrow spectrum for the radiation from low-energy electrons. The location of the  $f_{\max}$  of this type of burst (the typical cm- $\lambda$  C Type, spectrally) is highly dependent of the burst-region magnetic field.\*

\*For radiation from higher-energy (midly relativistic, 100 keV to 1 MeV or higher) electrons,  $f_{\max}$  is determined by both the magnetic field and the electron-energy range and spectrum; it is broadened and advanced to higher frequencies where the below- $f_{\max}$  attenuation phenomena are not as severe.<sup>7, 21, 21</sup> Synchrotron emission (from relativistic electrons) is inherently linearly polarized; on the sun, it is dispersed by the surrounding ionized medium into radiation that is mainly unpolarized but with some resultant circular polarization.

In a previous large-scale (2400-burst) survey, the upward shift of the  $f_{\text{max}}$ -band for intensity 3 bursts was established (the greatest percentage distribution for intensity 3 occurs at K band).<sup>7</sup> However, the distribution for intensities 1 and 2 remained the same (essentially as shown in Figure 2 of this report), peaking of C band. The flux-density levels of the 11 bursts with corresponding I and  $p_c$  trends were all intensity 1 or 2, hence, there should be no special tendency toward the higher microwave frequencies. Eight of the 11 bursts have their I- $p_c$  increase toward the low-frequency end (the C-band side) of the polarization-patrol range and only 3 toward the high-frequency side; this factor lends some further support to the "radiation from low-energy electrons" explanation described above.

With regard to the third result stated at the start of Section 4.2, eight bursts in Table 2 were found whose peak flux density spectra showed a reversal in the sense of circular polarization within the 5 to 9.4 GHz range. For each burst, the frequency of the circular-polarization crossover was estimated to the nearest gigahertz. In interpolating between the opposite sense measurements, the criterion used was that the "zero polarization" would occur nearer to the patrol frequency having the lesser polarization value. A careful estimation of the frequency of maximum I (for example, the spectral maximum frequency  $f_{\text{max}}$ ) was also made using both the I data from the polarization patrols and the flux density (total intensity) data from the regular Sagamore Hill patrols (which cover a wider range of frequencies). The information from both sources of I data was consistent, so there is high confidence in the total intensity results.

For all eight bursts, the interpolated circular-polarization crossover frequency agrees very closely with the interpolated frequency of maximum I — far more closely than both merely being within the 5 to 9.4 GHz range. See the remarks column of Table 2.

According to the Zheleznyakov theory of mode-coupling induced linear polarization, the greatest  $p_l$  should occur at the frequency where  $p_c = 0$ . The measurement of a  $p_l$  maximum at the crossover ( $p_c = 0$ ) frequency would certainly be strong evidence for the Zheleznyakov theory; however, there are many problems. Linear polarization could only be measured at 5 GHz, which is not necessarily where the crossover occurs. All previous investigations have indicated that even if there is some linear polarization in the solar burst radiation reaching the earth, it is very small. To be detected creditably, it would have to be above the threshold of the Q and U networks — estimated as about 3 percent or 2 sfu (whichever is larger). Under the circumstances, the measurement of any significant linear polarization near the crossover frequency for most of the bursts with a polarization-sense reversal would be a valuable finding.

The observational data (Table 2) show that only one of the eight bursts with  $p_c$  reversal had evidence of linear polarization at 5 GHz. This burst (number 29) was



a peculiar one; it apparently even had a circular-polarization reversal with time at 5 GHz. (This kind of burst is more suitable for individual analysis; it is a problem when it is the only one in a statistical study.) Overall, linear polarization was measured in 5 bursts out of the 45 listed in Table 2.

The statistical lack of measured linear polarization for the  $p_c$ -reversal bursts does not in itself rule out the Zheleznyakov hypothesis for solar bursts. It may be that, although  $p_l$  is present in the burst region, one cannot measure  $p_l$  at the earth with present instrumentation. The orientation angle ( $\chi$ ) of the linearly polarized burst emission could be dispersed by variations in the propagation-medium parameters above the burst region. Also, the 1 MHz bandwidths of the Q and U radiometric networks might be too wide (the  $f^{-2}$  dependent Faraday rotation of  $\chi$  could be significantly different at the upper and lower ends of the bandpass). Either or both of these effects could disperse linear polarization into apparent (as detected) randomly polarized radiation.

According to the Zheleznyakov mode-coupling theory, the transformation of  $p_c$  into  $p_l$  in the quasi-transverse (QT) region takes place without change in the overall polarization  $p$  or in the overall polarized intensity  $I_p$ . Since  $I = I_p + I_u$ , if by later dispersion some  $I_p$  (that is, the  $I_l$  part of  $I_p$ ) is converted into  $I_u$ , the total intensity  $I$  would remain the same. For illustrative purposes, consider hypothetically partially-polarized radiation at three frequencies, where  $I_p$  is left-circularly polarized at one end, right-circularly polarized at the other end, and linearly polarized in the middle, all according to the Zheleznyakov theory. If the emission-region total intensity  $I$  was larger at the upper or lower frequency, then the received  $I$  should also be larger at that frequency. However, the experimental result is that in eight out of eight cases of  $p_c$ -reversal bursts the maximum  $I$  always occurs at (or near) the middle frequency — an unlikely statistical outcome.

On the other hand, a theory discussed by Takakura<sup>12</sup>, Kai and others holds that the reversal of circular polarization sense in cm- $\lambda$  bursts may be explained by gyroresonance absorption. In contrast to the mode-coupling theory, this effect does not produce linear polarization. At the higher harmonics (the frequencies above  $f_{\max}$  relatively unaffected by the absorption), solar-burst emission is radiated in the extraordinary mode. In the lower frequencies where the gyroresonant absorption affects the first few harmonics severely (shaping the below- $f_{\max}$  portion of the spectrum), the resultant effect produces ordinary-mode radiation. This difference between ordinary and extraordinary mode radiation is manifested in the difference in the sense of polarization between the below- $f_{\max}$  and above- $f_{\max}$  radiation ( $f_{\max}$  is the frequency of maximum  $I$ ). Thus under the gyroresonance absorption theory, there is a clear reason for the maximum  $I$  to occur near (but not necessarily exactly at) the frequency where the propagation mode, and thereby the sense of circular polarization, changes.



It must be remembered that the polarization-reversal results discussed here offer only suggestive evidence. The usual caveat against drawing too sweeping a conclusion from so little data is obviously appropriate.

Although this report is about the study of circular polarization spectra, one brief point about the linear polarization observations might be noted here. For the five bursts in Table 2 where some linear polarization was apparently detected at 5 GHz, the only significant correspondence of other parameters listed in the table was the presence of a strong G-type spectral component (intensity 3 or the high end of the intensity 2 level). The composite (GC) spectra, however, is not unique to bursts with linear polarization; 21 other bursts also had GC spectra with no apparent  $p_l$  (to our present limit of detection). With lower-threshold Q and U observations of larger numbers of bursts, perhaps some linkage between the dm- $\lambda$  component and linear polarization in the cm- $\lambda$  component could be established. Such a linkage might be of help in establishing a theory to explain the often-observed joint presence of dm- $\lambda$  and cm- $\lambda$  components of microwave burst spectra.

Future solar-burst polarization studies will require a greater data base — more bursts and wider spectral coverage. Recording more bursts will require awaiting the return of the sunspot-maximum period. Wider spectral coverage would require setting up additional polarization patrols, with more funding for equipment and operation. *For a given fixed period*, high-resolution polarization observations (typically at one frequency) allow one to examine "bursts" or polarization anomalies to a much lower threshold. However, since high-resolution instruments are very costly, it is usually not feasible to direct their use to dedicated solar patrol for other than very short periods of time.

## References

1. Pawsey, J.L., and Bracewell, R.N. (1955) Radio Astronomy, Oxford Univer. Press, Oxford, p. 185.
2. Kraus, J.D. (1966) Radio Astronomy, McGraw-Hill, New York, p. 338.
3. Zheleznyakov, V.V. (1970) Radio Emission of the Sun and Planets, Permagon Press, Oxford, pp. 238-240.
4. Richards, D.W., and Straka, R.M. (1971) Solar polarization mapping at 7.8 GHz, Nature, Phys. Sci., 233:92.
5. Ishitsuka, M. (1975) Solar Patrol at 9400 MHz, Final Scientific Report, Instituto Geofisico del Peru, AFGL-TR-76-0050.
6. Castelli, J.P., Aarons, J., Guidice, D.A., and Straka, R.M. (1973) The solar radio patrol network of the USAF and its application, Proc. IEEE, 661:1307.
7. Guidice, D.A., and Castelli, J.P. (1975) Spectral distribution of microwave bursts, Solar Phys., 44:155.
8. Castelli, J.P., Guidice, D.A., and Aarons, J. (1975) Comparison of morphology and spectra of August 7, 1972 outburst at microwave and hard x-rays, presented at XVII Gen. Assembly of URSI, Lima, Peru, 11-15 August 1975.
9. Cohen, M.H. (1958) The Cornell radio polarimeter, Proc. IRE, 46:183.
10. Castelli, J.P., Guidice, D.A., Forrest, D.J., and Babcock, R.R. (1974) Solar bursts at  $\lambda = 2$  cm on July 31, 1972, J. Geophys. Res., 79:889.
11. Ko, H.C., and Chuang, C.W. (1976) Influence of the Solar Electron Energy Distribution on the Microwave Spectrum of Gyro-synchrotron Radiation, Ohio State University, AFGL-TR-76-0030.
12. Takakura, T. (1967) Theory of solar bursts, Solar Phys., 1:304.
13. Zheleznyakov, V.V. (1970) Radio Emission of the Sun and Planets, Permagon Press, Oxford, pp. 363-365.

14. Akabane, K. (1958) On elliptical polarization of solar radio outbursts at 9500 MHz, Publ. Astron. Soc. Japan, 10:99.
15. Magun, A., and Matzler, C. (1973) On the observation of solar microwave bursts, Solar Phys., 30:489.
16. Guidice, D.A., and Castelli, J. P. (1968) The Determination of Antenna Parameters by the Use of Extraterrestrial Radio Sources, Air Force Cambridge Research Laboratories, AFCRL-68-0231.
17. Guidice, D.A., and Castelli, J. P. (1971) The use of extraterrestrial radio sources in the measurement of antenna parameters, IEEE Trans. Aerospace and Elec. Sys., AES-7:226.
18. Castelli, J. P., and Guidice, D.A. (1975) Verification of solar patrol calibration at 15.4 GHz, Astrophys. Let., 16:71.
19. Sealy, S. (1950) Electron Tube Circuits, McGraw-Hill, New York, p. 206.
20. Castelli, J. P., and Guidice, D.A. (1972) On the Classification, Distribution and Interpretation of Solar Microwave Burst Spectra and Related Topics, Air Force Cambridge Research Laboratories, AFCRL-72-0049.
21. Castelli, J. P., and Guidice, D.A. (1976) Impact of current solar radio patrol observations, Vistas in Astronomy, 19:355.